Effect of P_2O_5 addition on the structural and spectroscopic properties of sodium aluminosilicate glass

Jia Ding (丁 佳)[1,2]*, **Youkuo Chen (陈尤阔)[1]**, **Wei Chen (陈 伟)[1]**, **Lili Hu (胡丽丽)[1]**, and **G. Boulon[3]**

[1]*Key Laboratory of Materials for High Power Laser, Shanghai Institute of Optics and Fine Mechanics,*
Chinese Academy of Sciences, Shanghai 201800, China

[2]*Graduate University of Chinese Academy of Sciences, Beijing 100049, China*

[3]*Physical Chemistry of Luminescence Materials, University of Lyon, UMR CNRS 5620, Villeurbanne 69622, France*

**Corresponding author: dingjiasiom@gmail.com*

The structural and spectroscopic properties of Na_2O-Al_2O_3-SiO_2-xP_2O_5 glasses ($x = 0$ to 7 mol%) are investigated. Both Raman and IR spectra reveal that discrete phosphate species ($[PO_4]^{-3}$, $[PO_3O_{1/2}]^{-2}$) with low polymerization degree can be formed in the silicate glass. These phosphate structures scavenge non-bridging oxygen ions and cations from the silicate network, resulting in an increase of the glass transition temperature. According to the Judd-Ofelt intensity parameters ($\Omega_2, \Omega_4, \Omega_6$) of Er^{3+}, the asymmetry of local environment around Er^{3+} becomes higher, and the bond covalency between Er^{3+} and O^{2-} decreases after P_2O_5 is introduced. In the emission spectra, photoluminescence intensity increases with increasing P_2O_5 concentration and the spectra are inhomogeneously broadened, revealing that the ligand electric field around Er^{3+} is dramatically changed, and the glass matrix becomes disordered.

OCIS codes: 160.2750, 160.5960.
doi: 10.3788/COL201210.071602.

Recently, phosphosilicate glass has gained considerable attention due to its applications in multiwavelength fiber laser and rare earth (RE) ion-doped optical glass fibers[1−4]. The addition of P_2O_5 improves the quantum efficiency of RE radioactive transitions[5−7], and the addition of phosphate also highly limits photo-darkening due to the formation of color centers[8,9].

In phosphosilicate glass research, the solubility of P_2O_5 in the silicate matrix is an inevitable problem[10]; moreover, the existence species of phosphate and their interaction with silicate network can greatly influence the structural and spectroscopic properties of the glass. To our knowledge, previous studies focus only on the phosphorous speciation changes in phosphosilicate glasses[11,12]. Few reports mention the host environment around the doped RE ions, the effect of phosphate addition on the emission spectrum, or the inner correlation between spectroscopic properties and the local structure.

In this letter, various amounts of P_2O_5 are introduced into the sodium aluminosilicate glass. The structural evolution induced by the addition of P_2O_5 is investigated based on Raman and infrared (IR) absorption spectra. Er^{3+} ions are added into the glass to investigate the environment of RE ions in our phosphosilicate glasses. With the absorption and emission spectroscopic analysis, the relationship between the glass structure and the spectroscopic properties is discussed.

A series of sodium aluminosilicate glass samples with the composition of $30Na_2O$-$5Al_2O_3$-$(65-x)SiO_2$-xP_2O_5-yEr_2O_3 ($x=0$, 1, 3, 5, and 7 mol%, $y=0$ and 0.75 mol%) were prepared by melt-quenching method. Analytical reagent grade powders of Na_2CO_3, $Al(OH)_3$, $Al(PO_3)_3$, SiO_2, and 99.99% high purity powders of Er_2O_3 were used as raw materials. Then, 50 g of well-mixed powders were melted in platinum crucible for 60 min in the temperature of 1 450 °C. The melt was quenched on a preheated steel plate and then annealed for 3 h at the temperature of 560 °C. The annealed glasses were cut and polished with the size of 20 × 20 × 3 (mm) for spectroscopic measurements.

The Raman spectra were measured using Renishaw inVia plus Raman spectroscopy excited by a He-Ne laser in the spectra range of $100-1500$ cm^{-1}. The IR absorption spectra were recorded by a Nexus FTIR spectrometer in the wavenumber range of $450-1400$ cm^{-1}, with a resolution of 2 cm^{-1}. The differential scanning calorimetry (DSC) was performed with an apparatus (409 PC/PG, NETZSCHSTA, Germany) under Ar atmosphere. Double-beam spectrophotometer (Lambda 900UV/VIS/NIR, Perkin-Elmer, USA) was used to record the absorption spectra in the wavelength range of $300-1700$ nm. The spectral resolution of the spectrophotometer was 1 nm. Emission spectra were measured with a spectrometer (FLS920, Fdinburg, UK). All the measurements were carried out at room temperature.

Figure 1 shows the Raman spectra of the silicate glass samples with different P_2O_5 concentrations in the range of $100-1500$ cm^{-1}. Figure 2 shows the IR absorption spectra of samples (with 0, 3, and 7 mol% P_2O_5). In the following discussion, the symbol Q^n represents a $[PO_4]$ tetrahedron with n bridging oxygen, and D^n represents a $[SiO_4]$ tetrahedron with n bridging oxygen. The major vibration modes in phosphosilicate glass and their corresponding Raman and IR bands are summarized in Table 1[13−18].

In the Raman spectra, the phosphate-free Na_2O-Al_2O_3-SiO_2 glass is characterized by the bonds at 570 and 1 096 cm^{-1}, which contribute to the symmetric stretching vibration mode of Si-O-Si[13,17] and the stretching vibration mode in D^3[16]. These bonds remain at relatively constant frequencies, but de-

Table 1. Raman IR Wavenumbers and Assignment of Vibration Modes

Vibrational Modes	Raman (cm^{-1})	
	Reference	This Work
PO_4^{3-} Sym. Stret.	940[13]	936
Si-O-Si Stret	1 200[13]	
Si-O-NBO Stret	1 100[13,14]	1 096
PO_4^{2-} Stret	440[13]	436
	490[13]	489
PO_4^{2-} Sym. Stret	1 024[13,18]	1 024
P-O-P Stret	640[13]	630

Vibrational Modes	IR (cm^{-1})	
	Reference	This Work
PO_4^{3-} Bend.	500 to 600[14,15]	574
Si-O-Si Stret	1 080[13,14]	1 075
Si-O-Si Rock	450 to 490[14]	491
Si-O-NBO Stret	1 020 to 1 040[14,16]	1 012 to 1 035
vSi-O$^-$	920[17]	920
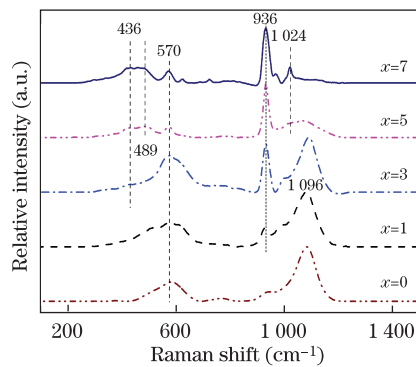
Fig. 1. Raman spectra of silicate glasses with x mol% P_2O_5 addition ($x = 0$, 1, 3, 5, and 7).
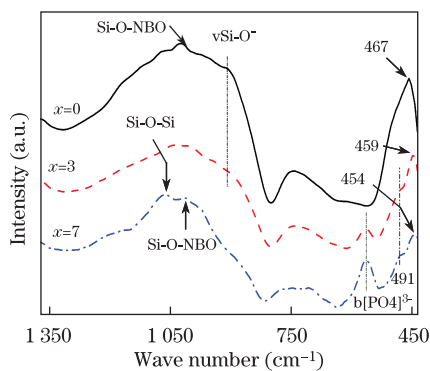
Fig. 2. IR absorption spectra of silicate glasses with x mol% P_2O_5 addition ($x = 0$, 3, and 7).

crease in relative intensities as P_2O_5 concentration increases. According to this phenomenon, it could be inferred that the phosphate exist as discrete phosphate structures that have not formed chemical bonds with the silicon-oxide tetrahedrons. Theoretically, the coupling effect between the phosphor-oxide tetrahedrons and the silicate network changes the silicate band frequencies,

resulting in a position shift for the characteristic peaks at 570 and 1 096 cm^{-1}, since $\nu \cong \sqrt{(\kappa/\mu)}$, where ν is the band frequency, κ is the effective force constant, and μ is the reduced mass of the structural unit.

After adding P_2O_5, a new characteristic band appears at 936 cm^{-1} belonging to the symmetric stretching of non-bridging oxygen ions in $Q^{0[13,14]}$. This feature indicates that phosphate structure-like orthophosphate ($[PO_4]^{-3}$) exists in the phosphosilicate glasses. As the P_2O_5 concentration increases, the intensity of this 936 cm^{-1} band becomes higher, while the intensities of the bands at 570 and 1 096 cm^{-1} decrease. This trend reveals that the quantity of $[PO_4]^{-3}$ increases; it also proves the fact the Raman scattering cross section of P-O is much bigger than that of Si-O[13]. For samples with 3, 5, and 7 mol% P_2O_5, there are corresponding bands around 436 cm^{-1} that show increasing intensities. These bands result from the stretching vibration mode in Q^1, which indicates there is phosphate structure-like pyrophosphate ($[PO_3O_{1/2}]^{-2})^{[13]}$. This phosphate structure could also be called phosphate dimer, because it is formed by the link of two phosphate monomers ($[PO_4]^{-3}$) through one bridging oxygen ion. Although the P_2O_5 is introduced in the form of metaphosphate ($[PO_2O_{2/2}]^-$), there are no characteristic peaks located at 1 190 and 1 250 cm^{-1} that represent the symmetric and asymmetric stretching vibration modes in Q^2 ($[PO_2O_{2/2}]^-$). This feature strongly proves that P_2O_5 mainly exist in the forms of Q^0 ($[PO_4]^{-3}$) and Q^1 ($[PO_3O_{1/2}]^{-2}$) in the silicate glasses instead of Q^2 ($[PO_2O_{2/2}]^-$); moreover, there is no chain-like phosphate structure but just phosphate monomer and dimer with lower polymerization degrees. Based on the structures of Q^0, Q^1, and Q^2, it is clear that both extra non-bridging oxygen ions and positive cations are needed in the transformation process from Q^2 to Q^0 and Q^1, and they could only be scavenged from the original silicate network. As the silicate network loses some of its non-bridging oxygen ions, the network becomes polymerized.

In the IR spectra, the bands located at 574 cm^{-1}, representing the bending vibration in $[PO_4]^{3-}$, prove the existence of phosphate in the glasses[14]. As P_2O_5 content increases, the intensity of the 574 cm^{-1} band also increases, implying that the P_2O_5 probably exists mainly as a discrete phosphate monomer in the sample. Meanwhile, the band formed due to the bending vibration in $[SiO_4]$ shows a red-shift from 467 to 454 cm^{-1}, indicating that there is a certain change in the original silicate network after the addition of $P_2O_5^{[19]}$. With increasing P_2O_5 concentration, the intensity of the band around 1 020 cm^{-1} due to the Si-O-NBO stretch vibration in $D^{3[14,16]}$ decreases. In the sample with 7 mol% P_2O_5, there is a new peak located in 1 090 cm^{-1}, which represents the Si-O-Si stretch vibration in $D^{4[13,14]}$, and its intensity is even higher than that of the 1 020 cm^{-1} peak. Meanwhile, there are new peaks located at 491 cm^{-1} due to the Si-O-Si rock vibration in the 3 and 7 mol% P_2O_5 samples. These features indicate that the number of the non-bridging oxygen in the Si network decreases with the addition of more P_2O_5.

In the spectra of the phosphate-free and 3 mol% P_2O_5 samples, the bands at 920 cm^{-1} represent the vibration

in the Si-O$^-$. With increasing P_2O_5 concentration, the intensity of the band declines and becomes too weak to be identified in the spectrum of the 7 mol% P_2O_5 sample. The decline of the Si-O$^-$ quantity in the silicate network also proves that Na$^+$ ions are scavenged by Q^0 and Q^1 from the silicate network.

Figure 3 shows the respective DSC curves of the samples with 0, 1, 3, 5, and 7 mol% P_2O_5. The glass transition temperatures of each sample are also shown.

The glass transition temperature largely depends on both the polymerization degree of the glass network and bond strength in glass[20]. Applying this to the phosphosilicate glasses in this research, these two factors are essentially interactive, because the glass network becomes more polymerized as a result of the change in bond species (Si-O-Na to Si-O-Si). It is reasonable to use the glass transition temperature to indicate the network polymerization degree in this system. With the increasing concentration of P_2O_5, the glass transition temperature increases by about 76 °C from 500.5 °C (0 mol% P_2O_5) to 576.1 °C (7 mol% P_2O_5). This change proves that the polymerization degree of the glass matrix increases with increasing P_2O_5 concentration, thus verifying the glass structure discussion above.

Figure 4 shows the absorption spectra of Er^{3+}-doped samples with 0, 1, 3, and 5 mol% P_2O_5 in the range of 300−1 700 nm. The corresponding wavelength assignments are shown in Fig. 4[21]. The Judd-Ofelt theory is used to calculate the J-O intensity parameters ($\Omega_{2,4,6}$) from the measured absorption spectrum[22,23]. The odd-symmetry crystal field terms
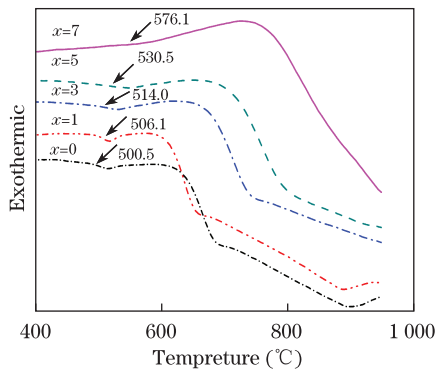

Fig. 3. DSC curves of silicate glasses with x mol% P_2O_5 addition (x=0, 1, 3, 5, and 7).
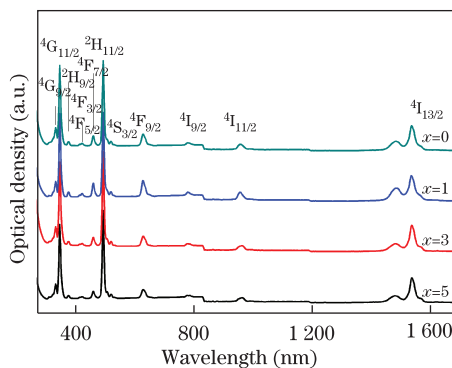

Fig. 4. Absorption spectra of silicate glasses with x mol% (x= 0, 1, 3, and 5) P_2O_5 addition.
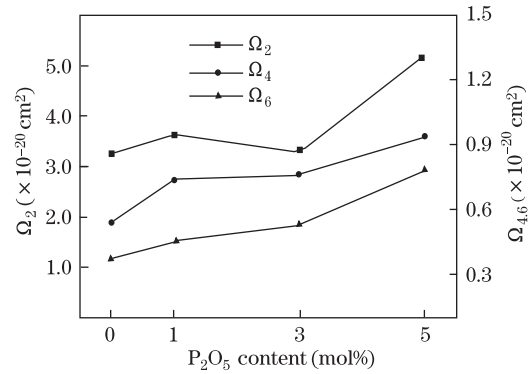

Fig. 5. Dependence of J-O intensity parameters ($\Omega_{2,4,6}$) of Er^{3+} ions on P_2O_5 addition.

of the glass host could influence the radioactive transition probabilities[21], and some structure information of the crystal field terms can be obtained from the comparison of the J-O parameters. The calculated results are shown in Fig. 5. The root-mean-square error is δ=0.6×10^{-6}, indicating the reliability of the calculation.

The value of Ω_2 is strongly dependent on the local environments of RE ions and is sensitive to the ligand asymmetry of host materials around such ions[21]. With higher asymmetry of the RE sites, the value of Ω_2 becomes higher. The increasing trend of Ω_2 value shown in Fig. 5 indicates that the host environment of the Er^{3+}ions becomes less ordered, and the ligand asymmetry becomes higher after introducing P_2O_5. The asymmetry of phosphate chain in the phosphate glass host is much higher than that of the silicate network in the silicate glass host. As discussed above, the mainly phosphate species are the phosphate monomers and dimers that have even higher asymmetry than the long phosphate chains and network. Network modifier ions M$^+$ (Na$^+$, K$^+$) and M^{2+} (Ca^{2+}) as well as the RE ions RE^{3+} (Er^{3+}) prefer to bond with non-bridging oxygen in phosphate structures rather than silicate structure; furthermore, the chemical bond of P-O-RE (M) is more stable than that of Si-O-RE (M)[24,25]. Thus, in the phosphate-bearing samples, Na$^+$ ions can migrate from the silicate network. As the two main reasons stated above, the Er^{3+} environment exhibits higher asymmetry and the site of Er^{3+} becomes increasingly disordered with more P_2O_5 concentrationd resulting in an increasing trend of Ω_2.

The spectroscopic intensity parameters Ω_4 and Ω_6 are closely related to the covalency between Er^{3+} and O^{2-} ions, and they increase when the covalency decreases[21,26]. In addition, the covalency between Er^{3+} and silicon-oxide tetrahedron is larger than that between Er^{3+} and phosphor-oxide tetrahedron[27]. A part of Er^{3+} cations coordinate with phosphate structures formed in the phosphate-bearing host, demonstrating that Er^{3+} ions are surrounded by O^{2-} ions incorporated with both Si^{4+} and P^{5+}. Figure 5 shows that the values of Ω_4 and Ω_6 both increase with increasing P_2O_5 concentration, indicating that the covalency between Er^{3+} and O^{2-} is decreased.

Figure 6 shows the emission spectra of silicate glasses with 0, 1, 3, and 5 mol% P_2O_5, all doped with 0.75 mol% Er$_2$O$_3$; the inset shows the calculated effective linewidth ($\Delta\lambda_{\text{eff}}$) and full-width at half-maximum
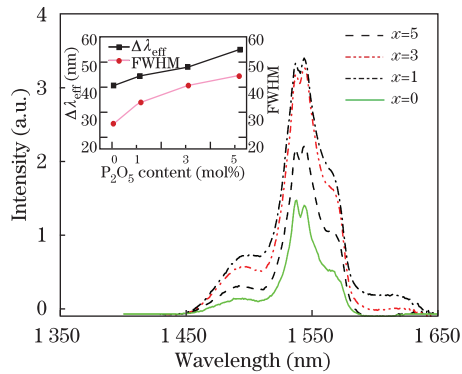
Fig. 6. Emission specra of samples with x mol% P_2O_5 addition (x=0, 1, 3, and 5). The inset shows the dependence of $\Delta\lambda_{\text{eff}}$ and FWHM of the glasses on P_2O_5 addition.

(FWHM) of the spectra. According to the emission spectra, $\Delta\lambda_{\text{eff}}$ can be calculated by $\Delta\lambda_{\text{eff}} = \frac{\int I_{\text{f}}(\lambda)\mathrm{d}\lambda}{I_{\text{f}}(\lambda_{\text{p}})}$[28], where $I_{\text{f}}(\lambda)$ is the intensity at the wavelength of λ, and $I_{\text{f}}(\lambda_{\text{p}})$ is the peak value of the emission spectra.

FWHM and $\Delta\lambda_{\text{eff}}$ both increase with increasing P_2O_5 concentration, indicating that there is inhomogeneous broadening in the spectra with increasing P_2O_5. Inhomogeneous broadening can result from the structural disorder of the glass, which causes differences in the ligand electric field effects at various sites of Er^{3+} ions, depending on the composition of the glass host[29]. The differences of the sites at which the Er^{3+} ions are located lead to different ligand electric field effects on the Er^{3+} ions, finally resulting in different Stark level splitting[30]. This is because the greater the disorder of the RE ion environment, the larger the inhomogeneous broadening there is.

The addition of P_2O_5 into silicate glasses changes the local environment of Er^{3+} ions. As discussed above, phosphate mainly exists in the form of $[PO_4]^{-3}$ and $[PO_3O_{1/2}]^{-2}$. RE ions (Er^{3+}) prefer to bond with non-bridging oxygen in phosphate species rather than that in silicate structure, for the ionic field strength of P^{5+} (43.2) is much larger than that of Si^{4+} (23.8)[31]. Therefore, the local ligand fields of Er^{3+} ions are greatly influenced by $[PO_4]^{-3}$ and $[PO_3O_{1/2}]^{-2}$, which are more disordered than the silicate network. This is the reason behind the inhomogeneous broadening of the Er^{3+} spectra with increasing P_2O_5 concentration.

In the phosphosilicate glass with a small amount of P_2O_5, P^{5+} ions do not substitute into Si^{4+} sites in silicate structures; instead, they form discrete phosphate species such as orthophosphate ($[PO_4]^{-3}$) and pyrophosphate $[PO_3O_{1/2}]^{-2}$. In this formation process, both non-bridging oxygen and Na^+ ions are obtained from the silicate network, resulting in the polymerization of the original silicate network and the increasing glass forming temperature. The asymmetry of the local environment around Er^{3+} becomes higher, and the bond covalency decreases between Er^{3+} and O^{2-} after introducing P_2O_5. The inhomogeneous broadening of the emission spectra indicates that P_2O_5 addition could greatly change the ligand electric field of Er^{3+} ions and make the site of RE ions disordered, which is in agreement with the structure characteristics deduced from the Raman and IR spectra.

In conclusion, the introduction of P_2O_5 leads to an ideal change for silicate glass, including the surrounding environment of RE ions as well as structural and the spectroscopic properties. This result provides effective guidance for future research.

References

1. T. Izumitani, M. Matsukawa, C. Hata, K.Tanaka, and H. Toratani, Laser Induced Damage in Optical Materials **752,** 13 (1988).
2. Y. Chen, L. Wen, L. Hu, W. Chen, Y. Guyot, and G. Boulon, Chin. Opt. Lett. **7,** 56 (2009).
3. J. Wang, Z. Luo, Z. Cai, M. Zhou, C. Ye, and H. Xu, IEEE. Photon. J. **3,** 633 (2011).
4. M. Melkumov, A. Laptev, M. Yashkov, N. Vechkanov, A. Guryanov, and I. Bufetov, Inorg. Mater. **46,** 299 (2010).
5. K. Arai, H. Namikawa, K. Kumata, T. Honda, Y. Ishii, and T. Handa, J. Appl. Phys. **59,** 3430 (1986).
6. K. Arai, H. Namikawa, Y. Ishii, H. Imai, H. Hosono, and Y. Abe, J. Non-Cryst. Solids **95&96,** 609 (1987).
7. S. Tanabe, J. Non-Cryst. Solids **259,** 1 (1999).
8. S. Jetschke, S. Unger, A. Schwuchow, M. Leich, and J. Kirchof, Opt. Express **16,** 15540 (2008).
9. M. Engholm and L. Norin, Opt. Express **16,** 1260 (2008).
10. S. Liu, Y. Zhang, W. He, and Y. Yue, J. Non-Cryst. Solids **357,** 3897 (2011).
11. B. Mysen, Am. Mineral. **81,** 1531 (1996).
12. M. J. Toplis and T. Schaller, J. Non-Cryst. Solids **224,** 57 (1998).
13. C. Nelson and D. R. Tallant, Phys. Chem. Glasses **25** 31 (1984).
14. H. Aguiar, J. Serra, P. González, and B. León, J. Non-Cryst. Solids **355,** 475 (2009).
15. C. Y. Kim, A. E. Clark, and L. L. Hench, J. Biomed. Mater. Res. **26,** 1147 (1992).
16. M. Kawashita, F. Miyaji, T. Kokubo, G. H. Takaoka, I. Yamada, Y. Suzuki, and M. Inoue, J. Non-Cryst. Solids **255,** 140 (1990).
17. T. Fuss, A. Mogus-Milankovic, C. S. Ray, C. E. Lesher, R. Youngman, and D. E. Day, J. Non-Cryst. Solids **352,** 4101 (2006).
18. D. R. Tallant and C. Nelson, Phys. Chem. Glasses **27** 75 (1986).
19. L. Luo and J. Li, J. Non-Cryst. Solids. **112,** 215 (1989).
20. L. Chen, C. Yu, L. Hu, and W. Chen, J. Chinese Ceramic Society **38,** 11 (2010).
21. H. Desirena, E. De la Rosa, L. A. Diaz-Torres, and G. A. Kumar, Opt. Mater. **28,** 560 (2006).
22. B. R. Judd, Phys. Rev. **127,** 750 (1962).
23. G. S. Ofelt, J. Chem. Phys. **37,** 511 (1962).
24. B. O. Mysen, F. J. Ryerson, and D. Virgo, Am. Mineral. **66,** 106 (1981).
25. D. Li, M. E. Fleet, G. M. Bancroft, M. Kasrai, and Y. Pan, J. Non-Cryst. Solids **188,** 181 (1995).
26. S. Tanabe, T. Ohyagi, S. Todoroki, T. Hanada, and N. Soga, J. Appl. Phys. **73,** 8451 (1993).
27. F. Gan, *Optical and Spectroscopic Properties of Glass* (Springer-Verlag, Berlin Heidelberg, 1992).
28. J. H. Campbell and T. I. Suratwala, J. Non-Cryst. Solids, **263,** 318 (2000).
29. Y. Fang, L. Hu, M. Liao, and L. Wen, J. Alloys Compd. **457,** 19 (2008).
30. W. J. Miniscalco, J. Lightwave Technol. **9,** 234 (1991).
31. M. Mirsaneh, I. M. Reaney, and P. V. Hatton, J. Non-Cryst. Solids **354,** 3362 (2008).